МОЛЕКУЛЯРНАЯ БИОЛОГИЯ, 2011, том 45, № 3, с. 503–509

МОЛЕКУЛЯРНАЯ БИОЛОГИЯ
КЛЕТКИ

UDC 631.524.82

EXPRESSION PATTERNS OF TWO *Arabidopsis* ENDO-β-1,4-GLUCANASE GENES (*At3g43860*, *At4g39000*) IN REPRODUCTIVE DEVELOPMENT

© 2011 Xiao-Jun Xie, Jun-Jun Huang, Huan-Huan Gao and Guang-Qin Guo*

Institute of Cell Biology, Lanzhou University, Tanshui road 222, Lanzhou 730000, Gansu, PR China

Received June 08, 2010
Accepted for publication August 24, 2010

Endo-β-1,4-D-glucanases (EGases) are a widespread and vital group of glycosyl hydrolases that generally break the β-1,4-glucosyl linkages. Studies of plant EGases have mainly been concentrated on vegetative growth, while little is currently known about their role in reproductive processes. Using the GUS reporter aided analysis of promoter activities, we identified the expression patterns of two putative *Arabidopsis* EGases genes (*At3g43860* and *At4g39000*) whose promoters conferred specific localization of the GUS activity in reproductive organs. We found that *At3g43860*, which is similar to KOR in its protein structural organization, is expressed in mature pollen and the pollen tube, implying that it may have a role in pollen and pollen tube growth. *At4g39000* was found to be activated in the developing ovules and seeds, especially at the micropylar end of the inner integuments and nucellus in a proximal-distal pattern. Our results suggested that the two EGases play specific roles in Arabidopsis sexual reproduction.

Keywords: **Endo-β-1,4-D-glucanase, GUS, integument, pollen, pollen tube**

The growth of a plant cell exhibits dynamic changes in the cell wall structure and composition. The plant cell wall is a flexible network of polysaccharides in which the major components, the crystalline cellulose microfibrils, are mainly tethered by xyloglucans and embedded in a matrix of complex polysaccharides [1]. According to the development cues, plant cells modify their wall by depositing new wall materials such as cellulose and hemicellulose [2] and by secreting wall modifying molecules such as carbohydrate-active enzymes [3], expansins [4] and reactive oxygen species [5].

Plant endo-β-1,4-D-glucanases (EGases) are vital carbohydrate-active enzymes. They generally cleave the internal β-1,4-glucosyl linkages which are one of the principle covalent bonds engaging in the construction of cell wall materials including cellulose, xyloglucan, β-1,3-1,4-glucans [6]. The biochemical properties of plant EGases confer them the ability to modify the plant cell wall, and thus, they should play important roles in plant development. Many studies have linked plant EGases to cell elongation [7, 8], cell expansion [9, 10], cell separation [11, 12], ripening [10] and pathogenesis [13].

The essential role of plant EGases makes them widespread in the plant kingdom. Blast searches in the EST (expressed sequence tags) databases showed the presence of EGase-like sequences in a wide variety of plants [14]. Moreover, analysis of the complete plant genome sequences has revealed the existence of a relatively large multigene family of EGases that can be subdivided into three distinct structural subclasses: Class A (membrane anchored), Class B (secreted) and Class C (secreted and with a carbohydrate binding module, CBM49) [15].

In *Arabidopsis*, the EGases gene family contains 25 members. Some members of the family have been studied, as for example the membrane anchored (Class A) EGase KOR1 (At5g49720). The *kor1* mutant has defects in cell elongation and cytokinesis, and it has been postulated that the KOR1 protein is involved in cellulose synthesis by trimming sterol residues from nascent glucan primers or by trimming out-of-register glucans to aid crystallization of the microfibril [1, 7, 8, 16]. Furthermore, two additional membrane-anchored Class A EGase genes (*KOR2* and *KOR3*) were characterized [17]. The expression profile of *KOR2* and *KOR3* showed that they have greatly distinct expression patterns from that of *KOR1*, and they are expressed in cell types at time points when cell wall assembly is likely to occur [17]. Shani et al. [18–20] and Tsabary et al. [21] examined a Class B EGase At1g70710 (AtCel1) and presented indirect evidence that it functions during wall deposition and integration. Moreover, At1g70710 was proved to differentially target the cell wall of specific cells, such as the developing xylem and epidermal cells of the stem [20]. Del Campillo et al. [22] showed that another Class B EGase gene *At1g22880* (*AtCel5*) was responsible for the sloughing of root cap cells and thus provided a new molecular tool for studying root cap development and root cap cell-cell separation. However, the functions of the remaining proteins in this family are unknown.

So far all of the known functions of the EGases mentioned above were related to vegetative development, but

* E-mail: gqguo@lzu.edu.cn

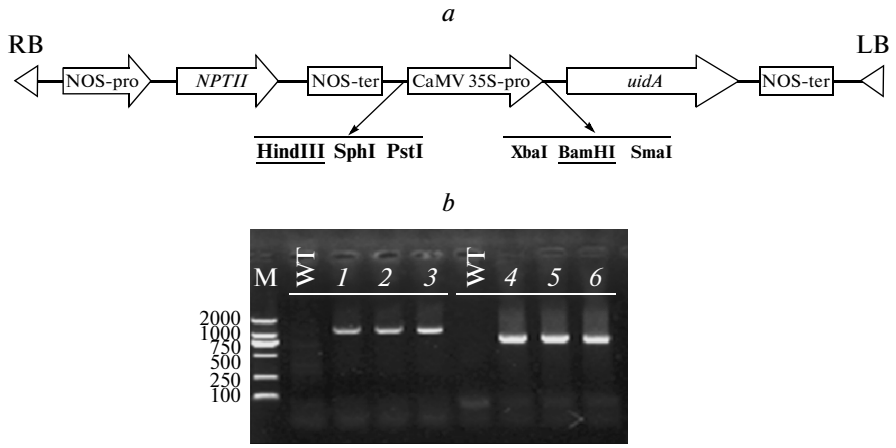

Fig. 1. *a* – Schematic diagram of the T-DNA region of the binary plasmid pBI121. LB and RB: left and right borders, respectively; CaMV 35S-pro: CaMV 35S promoter; NOS-pro: nopaline synthase promoter; NOS-ter: nopaline synthase terminator; *NPTII*: neomycin phosphotransferase II; *uidA*: β-gluduronidase reporter gene; arrows indicate the multi-cloning sites at both sides of CaMV 35S-pro; the underline indicates HindIII and BamHI sites used for the directed cloning of the specific promoters. *b* – Verification of transgenic plants by PCR assay. M – DNA marker; WT – wild type Col-0; lane *1–3*: *At4g43860-GUS* plants with positive GUS activity; lane *4–6*: *At4g39000-GUS* plants with positive GUS activity.

little is known about their role in reproductive development, although the cell wall undergoes significant changes in both the vegetative and the reproductive development. Here we report two EGase genes (*At3g43860* and *At4g39000*) whose promoters were specifically activated during reproductive development. Both At3g43860 and At4g39000 are putative EGases with a predictable glycosyl hydrolase family 9 (GH9) catalytic domain [6]. Moreover, At4g39000 also has a predictable N-terminal signal peptide and so is likely to be soluble and secreted, while At3g43860 has a predictable N-terminal transmembrane domain without a signal peptide. According to their structural organization, At3g43860 and At4g39000 belong to the membrane anchored Class C and the secreted Class B, respectively [6]. We provide a detailed tissue specific analysis of their gene expression, and the results suggest that they may have essential roles in reproductive development.

EXPERIMENTAL

Plant material and growth conditions. *A. thaliana* ecotype Col-0 was used in all experiments. Seeds were surface sterilized, rinsed in sterile water five times and sowed on solid MS plates [23] supplied with 1% sucrose. After treatment for three days at 4°C the plates were moved into the growth chamber with a light/dark cycle of 16 h/8 h (21 ± 2°C, 30 μmol m^{-2} s^{-1}). Seven days after germination, the seedlings were subjected to analysis or transplanted into soil for further growth in the same conditions.

Promoter-GUS fusion constructs. Promoters were amplified and fused to the *uidA* gene by replacement of the CaMV35S promoter of pBI121 [24] (Fig. 1*a*). Primer pairs used for PCR of each promoter are listed in Table 1. The amplified promoter fragments were separately cloned into a pUCm-T vector and conformed by DNA sequencing, after that they were further subcloned into pBI121 between the HindIII and BamHI sites (Fig. 1*a*, Table 1). The constructed vectors were introduced into *Arabidopsis* via *Agrobacterium tumefaciens* (GV3101) by the floral dip method [25]. The transformed seedlings were selected by germinating in the presence of 50 mg/L kanamycin and finally confirmed by positive PCR (Fig. 1*b*) on genomic DNA with primers (Table 1) specific for each promoter and *uidA* gene.

GUS staining. For promoter-GUS localization tissues were stained according to Jefferson et al. [24]. The tissues were fixed in 90% (v/v) ice-cold acetone for

Table 1. Primer pairs used for PCR amplifications

Primer names	Primer sequences [5' ⟶ 3']	Product size, bp
At3g43860F	AACAAGCTT[HindIII]AAAGGATTTGTAAACTTATCG	1953
At3g43860R	TTGGATCC[BamHI]GATTTCAAAAGTTATGTTTGTAA	
At4g39000F	ACAAAGCTT[HindIII]TTAAGTTCCAAGAGTATG	2104
At4g39000R	CGGGATCC[BamHI]TTATTAGGACTTGGTGAG	
At3g43860GUS-F	CATCCAGCTCACAGCCTAAT	1139
At4g39000GUS-F	ATAATAAAGAAGAGGCATCCCG	780
GUS-R	GGTTGGGGTTTCTACAGGACG	–

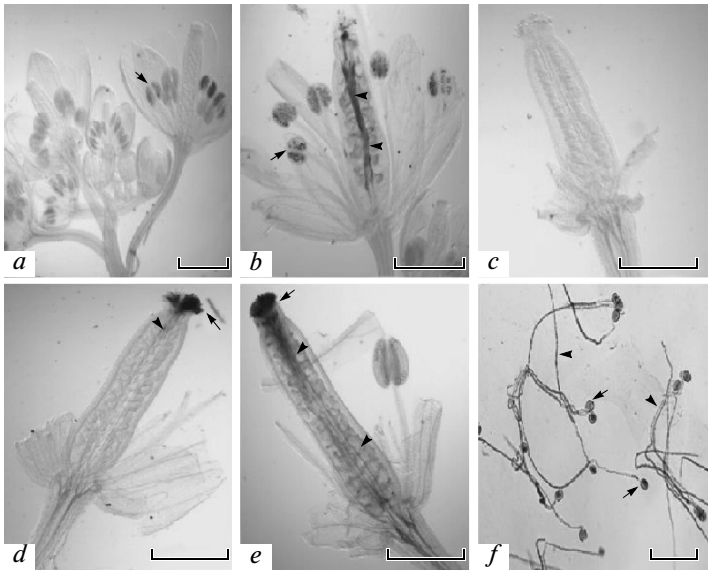

Fig. 2. Localization of *At3g43860-GUS* expression. *a* – No GUS staining in flower buds from floral stage 1 to 11 and until the beginning of stage 12, staining was observed in anthers (arrow). *b* – GUS activity was observed in pollens (arrow) and pistil (arrow head) at stage 14. *c* – No GUS staining was detected in emasculated *At4g43860-GUS* pistil pollinated by WT pollens. *d, e* – Emasculated WT pistil pollinated by *At4g43860-GUS* pollens (arrow). GUS activity was observed 4 h after pollination (*d*) and 24 h after pollination (*e*) in the female reproduction tract (arrow head). *f* – *In vitro* grown *At4g43860-GUS* pollen tubes: pollen grains (arrows), pollen tubes (arrow heads). Floral stages are in accordance with those described by Smyth et al. [28]. *a–e* – Bar = 1 mm; *f* – Bar = 30 μm.

20 min, rinsed twice in GUS working solution (50 mM sodium phosphate buffer, 0.5 mM $K_3Fe(CN)_6$, 0.5 mM $K_4Fe(CN)_6$, 10 mM Na_2EDTA, 0.1% (v/v) Triton X-100, pH7.0) and then submerged in 1 mg/ml 5-bromo-4-chloro-3-indolyl-β-D-glucuronic acid (X-gluc) dissolved in working solution. After vacuum infiltration, the tissues were incubated at 37°C until blue color was visible. The staining solution was removed and the tissues were washed with several changes of 95% ethanol until clear. Then, the tissues were moved into 75% ethanol and incubated at room temperature for 15 min, followed by treatment with 0.24 M HCl in 20% methanol at 37°C for 15 min. The solution was replaced by 7% NaOH in 60% ethanol. After incubation at room temperature for 15 min, the tissues were rinsed in ethanol series (40, 20, 10, 5%) for 5 min each and finally cleared with Hoyer's solution (7.5 g gum Arabic, 100 g chloral hydrate, 5 ml glycerol, 60 ml water).

In order to GUS stain the ovules and seeds, developing carpels/siliques were dissected to expose the ovules or seeds, vacuum infiltrated and incubated in GUS working solution with 1 mg/ml X-gluc at 37°C overnight. Then, individual ovules or seeds were dissected from the pistils/siliques and mounted in Hoyer's solution. Images were photographed with a Digital Camera under the Zeiss stereoscope or microscope. At least three independent T1 lines were examined to ensure reproducibility. Staining patterns were compared with the microarray data.

Pollen tube growth assay. For the *in vitro* culture pollen grains from open flowers were spread into a petri dish containing solid pollen germination medium (18% sucrose, 0.01% Boric acid, 1 mM $MgSO_4$, 2 mM $CaCl_2$, and 0.5% agarose, pH 7.0, [26, 27]) and incubated at 21 ± 2°C overnight. Germinated pollen tubes were directly submerged into the GUS working solution containing 1 mg/ml X-gluc. After being incubated at 37°C overnight, pollen tubes were then placed in a tiny drop of Hoyer's solution on the slide and mounted. Images were captured as described above.

Microarray data collecting, processing and analysis. Microarray data for the expression of each gene were retrieved from http://bbc.botany.utoronto.ca/efp/cgi-bin/output/efp-b7uJo9.html for *At3g43860* and http://bbc.botany.utoronto.ca/efp/cgi-bin/output/efp-vwMe2p.html for *At4g39000*, respectively. This data was processed and analyzed using the program Origin 8 (version 8.0, Microcal Software, Inc., USA).

RESULTS

Promoter of At3g43860 was active specifically in pollen and pollen tubes

To analyze tissue and cell specific expression of *At3g43860*, a promoter-reporter fusion (*At3g43860-GUS*) was constructed between an upstream DNA segment (1953 bp) of the *At3g43860* gene and the *Escherichia coli* β-glucuronidase (*uidA*) gene [24]. We adopted the flower developmental stages used by Smyth et al. [28]. *At3g43860-GUS* plants showed GUS staining exclusively in pollen during floral stages 12 to 14 (Fig. 2*a*,*b*) and in the pistil at stage 14 (Fig. 2*b*). Under the current staining conditions, we have not detected blue GUS activity in other tissues (data not shown).

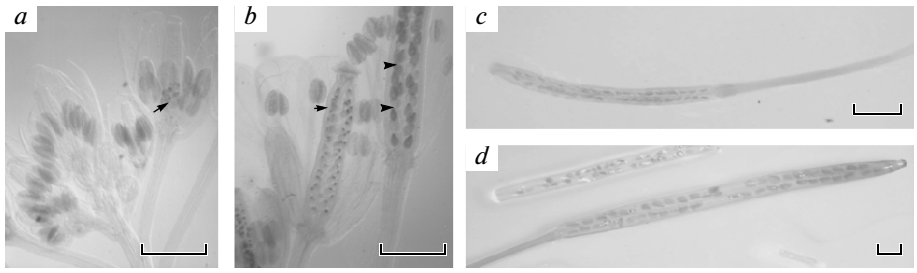

Fig. 3. Localization of *At4g39000-GUS* expression. *a* – GUS staining was observed in anthers from floral stage 10 to 11 and GUS activity in the ovules emerged at approximately stage 12 (arrow). *b* – A stage 13 pistil was full of GUS staining ovules (arrow) and GUS activity was also observed in later stages (arrow heads). *c* – A silique 2 days after pollination (DAP). *d* – A silique at 5 DAP. Bar = 1 mm.

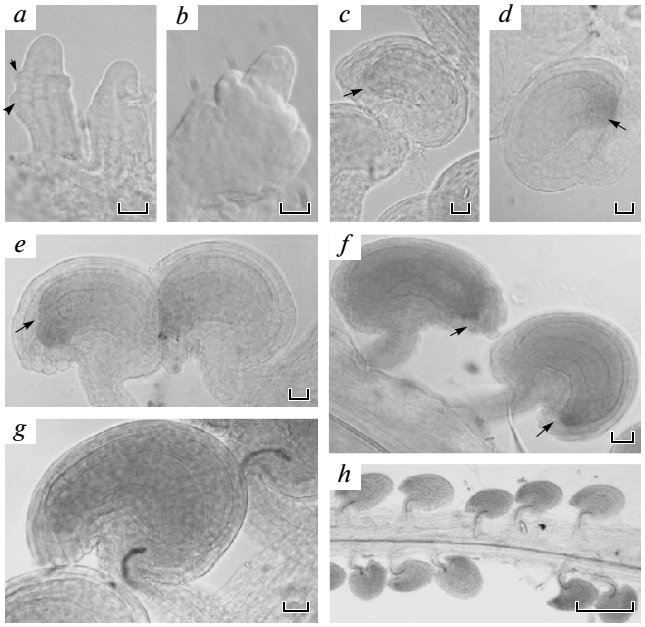

Fig. 4. Expression patterns of *At4g39000-GUS* in the developing ovules. *a* – An ovule (left) at stage 2-III. Both inner (arrow) and outer (arrow head) integuments initiate. *b* – An ovule at stage 2-III/2-IV. *c* – An ovule at early stage 3-IV with the inner integuments (arrow) nearly surrounding the nucellus. *d–f* – Ovules at approximately stage 3-IV to 3-V. Arrows indicate the micropyle. *g* – A mature ovule at around stage 3-VI. *h* – Ovules attach to the placenta at stage 3-V or 3-VI. Stages are in accordance with those described by Schneitz et al. [29]. *a–g* – Bar = 10 μm; *h* – Bar = 100 μm.

In order to determine whether the GUS staining in the pistil was caused by GUS expression in the pollen tube, in the female reproduction tract (FRT) or both, we conducted the emasculation and cross-pollination experiments. The emasculated *At3g43860-GUS* flowers pollinated by WT pollens showed no GUS staining in the pistil (Fig. 2*c*) while the emasculated WT flowers pollinated by *At3g43860-GUS* pollens showed GUS staining in the pistil (Fig. 2*d*,*e*). In addition, GUS activity has not been found in emasculated pistils of *At3g43860-GUS* plants without pollination (data not shown). We also conducted the *in vitro* pollen germination experiment to verify the GUS activity of the promoter (Fig. 2*f*). Both *in vitro* and *in vivo* experiments showed that the promoter of *At3g43860* was active in the pollen tube, but not in FRT. Thus, GUS staining in the pistil (Fig. 2*b*) was caused by the GUS activity in the pollen tubes rather than in FRT.

The localization of At4g39000-GUS activity in ovules and seeds

An upstream DNA segment (2104 bp) of the *A4g39000* gene was fused to the *uidA* gene to make the *At4g39000-GUS* fusion. Examination of *At4g39000-GUS* expression showed staining in anthers, ovules and early seeds (Fig. 3–5). The GUS expression in anthers started at stage 10, spanned during stage 11 and declined late in stage 12 (Fig. 3*a*). The GUS expression in ovules started at the beginning of stage 12 and persisted throughout the early stages of seed development (Fig. 3*a–d*).

A more detailed analysis was carried out on the ovules and seeds of *At4g39000-GUS* plants. Ovule developmental stages were determined according to Schneitz et al. [29]. No GUS staining was found in ovules at early stages (Fig. 4*a*,*b*). The expression of *At4g39000-GUS* started at stage 3-IV when the inner integuments almost surrounded the nucellus (Fig. 4*c*). The GUS staining at this stage was exclusively localized in the inner integuments at the

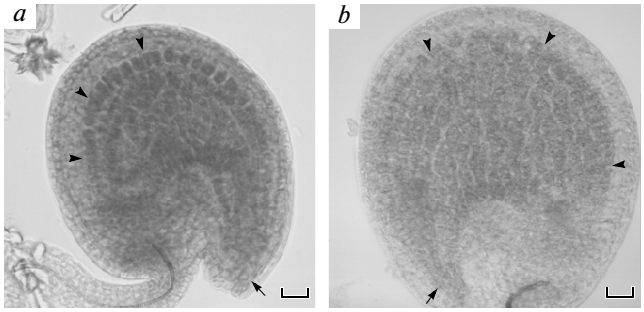

Fig. 5. Expression patterns of *At4g39000-GUS* in developing seeds. *a* – A seed at about 2 DAP with GUS staining significantly high in the endothelium. *b* – A seed at about 3 DAP with decreased GUS staining. Arrow indicates the micropyle and arrow heads indicate the endothelium. Bar = 50 μm.

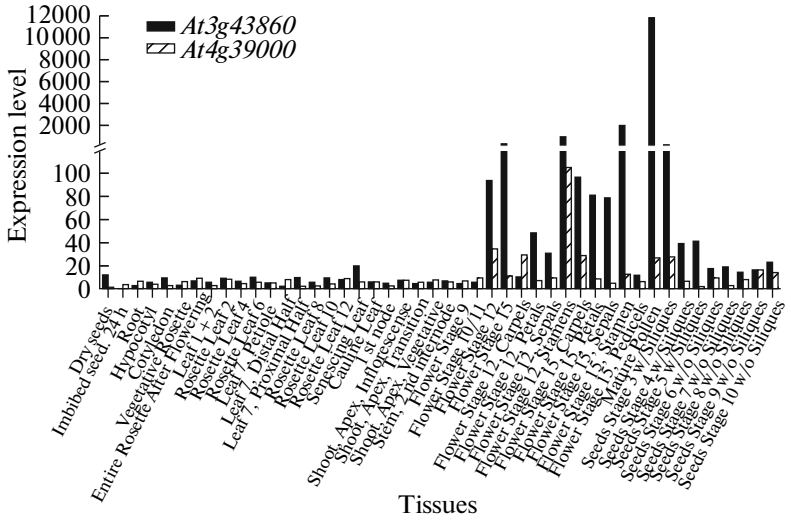

Fig. 6. Expression profiles of *At3g43860* and *At4g39000*.

micropylar pole (Fig. 4*c*). As the ovule continued to develop, GUS signal became stronger at the micropylar end of both the inner integuments and the nucellus, but was still very weak in the outer integuments (Fig. 4*d*,*e*). The maximum of GUS activity at the micropylar end of the inner integuments and the nucellus could be detected up to the late stage 3-V (Fig. 4*c*–*f*,*h*), while in the mature ovule at stage 3-VI (Fig. 4*g*), the distribution of the GUS signal became less polarized and spread throughout the ovule.

During early stages of the post-fertilization development, we could detect expression of *At4g3900-GUS* in the whole seed (Fig. 5*a*), staining being especially strong in the endothelium and the innermost cell layer of the seed coat. The GUS activity declined in the subsequent stages (Fig. 3*c*,*d*, Fig. 5*b*).

Comparison of the GUS expression patterns with microarray data

To validate our *GUS* expression results, we compared them with the microarray data (Fig. 6, Table 2). We mainly used the microarray data mining tool *Arabidopsis eFP Browser* in this study [30] for exploring *Arabidopsis* microarray data of the two genes. We also explored other microarray data, such as ovule transcriptome [31] and transmitting tract transcriptome [32] to complement the data from eFP.

Both the GUS staining data and the microarray data show that the two genes were active specifically in the reproductive processes (Fig. 2–6, Table 2). Expression patterns for *At3g43860-GUS* were essentially identical to the microarray results [30]. Both results showed that *At3g43860* was active in pollen and the pollen tube (Fig. 2, Fig. 6). While we did not find any GUS activity in sepals and petals by staining, the microarray data indicates such expression of *At3g43860*, suggesting that GUS-staining may be not enough sensitive or that other factors may be engaged in the expression regulation of *At3g43860*. Expression patterns for *At4g39000* were also identical to microarray data in stamens, ovules and seeds [30, 31] (Fig. 6, Table 2). Compared with the microarray data promoter-GUS staining provided a more detailed expression pattern of *At4g39000*.

DISCUSSION

Many carbohydrate-active enzymes have been implicated in pollen germination and pollen tube growth [32],

Table 2. Identical expression patterns indicated by GUS assay and microarray analysis

Gene name	GUS assay	Microarray data
At3g43860	pollen (stage 12–13); pollen tube (stage 13–14)	tricellular pollen, mature pollen and pollen tube [30]
At4g39000	stamen (stage 10–14); ovule (stage 12–13); seeds	stamen and pistil and seeds [30], ovules (late floral stage 11 to stage 13) [31]

and most of them, such as VANGUARD1, a pectin methylesterase involved in pollen tube growth and enhancement of transmitting tract degradation [33] are secreted. At3g43860 is a putative membrane-anchored EGase and is likely to be localized at the surface of the pollen tube. As mentioned above, At3g43860 belongs to Class C of GH9, four members of which are found in *Arabidopsis*, and the other three are: KOR1, KOR2 and KOR3. KOR1 was implicated in cellulose biosynthesis in all types of cells in *Arabidopsis* except for the tip-growing cells, including root hairs and pollen tubes [7, 34]. The expression of KOR2 and KOR3 were not detected in pollen and pollen tubes [17]. Thus, taken our results together, At3g43860 may be the only membrane-anchored EGase that is expressed in mature pollen and pollen tubes.

Interestingly, although At3g43860 is similar to KOR proteins in its structural organization and therefore belongs to Class C, phylogeny analysis showed that At3g43860 was more divergent to the other KOR proteins, but closely related to At4g23560, a Class B member [14]. Indeed, the gene pair, *At3g43860/At4g23560*, were identified in older sets of duplicated blocks [14]. It seems that the membrane-anchored EGase At3g43860 may arise independently from other KOR proteins. In other words, the ancestor of At3g43860 may have been a Class B member which gained a trans-membrane region in the evolution process. Thus, whether At3g43860 is involved in cellulose synthesis just as the other KOR proteins or it has other roles, such as facilitating the penetration of the pollen tube through FRT, still need a more detailed investigation.

Like most angiosperms, *Arabidopsis* ovules have two integuments, the inner and the outer ones, which grow to enclose the nucellus. Both integuments show similar developmental polarity, although they have different evolutionary origin. However, the mechanism for the proximal-distal patterning in the integuments is ambiguous, while the abaxial-adaxial patterning in both integuments and the proximal-distal patterning in the nucellus have been better established [35–37]. The localization of *At4g39000-GU*S showed a proximal-distal pattern in the ovule, and its expression was coincident with the rapid growth of the inner integument at the micropylar pole during ovule development. Its proximal-distal pattern emerged at stage 3-IV when the inner integument nearly enclose the nucellus and was maintained until stage 3-VI when the ovule matured. Moreover, this pattern was similar to that of some specific AGPs (arabinogalactan proteins) in the ovule, which are critical signal molecules in plant development [38]. Thus, in addition to a role in the development of integument, *At4g39000* could serve as a marker for analysis of the proximal-distal patterning in inner integument. Moreover, we also detected that the GUS expression was especially strong in endothelium in the early seeds, suggesting that At4g39000 may be involved in the early development of the endothelium.

In conclusion, we showed detailed spatial and temporal expression patterns of two *Arabidopsis* EGases genes (*At3g43860*, *At4g39000*) during pollen, ovule and seed development. Our results suggested specific roles for the two EGases in *Arabidopsis* sexual reproduction. Further studies should use their related mutants to reveal their likely physiological and developmental functions.

ACKNOWLEDGMENTS

We would like to thank the Ministry of Sciences and Technology (973 project no. 2007CB108700) and the National Science Foundation of China (no. 30330310) for support to Guang-Qin Guo.

REFERENCES

1. Cosgrove D.J. 2005. Growth of the plant cell wall. *Nature*. **6**, 850–861.
2. Lerouxel O., Cavalier D.M., Liepman A.H., Keegstra K. 2006. Biosynthesis of plant cell wall polysaccharides—A complex process. *Curr. Opin. Plant Biol*. **9**, 621–630.
3. Minic Z., Jouanin L. 2006. Plant glycoside hydrolases in cell wall polysaccharide degradation. *Plant Physiol. Biochem*. **44**, 435–449.
4. McQueen-Mason S.J., Cosgrove D.J. 1995. Expansin mode of action on cell walls. Analysis of wall hydrolysis, stress relaxation, and binding. *Plant Physiol*. **107**, 87–100.
5. Foreman J., Demidchik V., Bothwell J.H., Mylona P., Miedema H., Torres M.A., Linstead P., Costa S., Brownlee C., Jones J.D., Davies J.M., Dolan L. 2003. Reactive oxygen species produced by NADPH oxidase regulate plant cell growth. *Nature*. **27**, 442–446.
6. Urbanowicz B.R., Bennett A.B., del Campillo E., Catala C., Hayashi T., Henrissat B., Hofte H., McQueen-Mason S.J., Patterson S.E., Shoseyov O., Teeri T.T., Rose J.K.C. 2007. Structural organization and a standardized nomenclature for plant endo-1,4-beta-glucanases cellulases of glycosyl hydrolase family 9. *Plant Physiol*. **144**, 1693–1696.
7. Nicol F., His I., Jauneau A., Vernhettes S., Canut H., Hofte H. 1998. A plasma membrane–bound putative endo-1,4-β-D-glucanase is required for normal wall assembly and cell elongation in *Arabidopsis*. *EMBO J*. **17**, 5563–5576.

8. Zuo J., Niu Q.W., Nishizawa N., Wu Y., Kost B., Chua N.H. 2000. KORRIGAN, an *Arabidopsis* endo-1,4-beta-glucanase, localizes to the cell plate by polarized targeting and is essential for cytokinesis. *Plant Cell.* **12**, 1137–1152.
9. Carpita N.C., Gibeaut D.M. 1993. Structural models of primary cell walls in flowering plants. Consistency of molecular structure with the physical properties of the walls during growth. *Plant J.* **3**, 1–30.
10. Rose J.C., Bennett A.B. 1999. Cooperative disassembly of the cellulose-xyloglucan network of plant cell walls. Parallels between cell expansion and fruit ripening. *Trends Plant Sci.* **4**, 176–183.
11. Roberts J.A., Whitelaw C.A., Gonzalez-Carranza Z.H., McManus M.T. 2000. Cell separation processes in plants. Models, mechanisms and manipulation. *Ann. Bot.* **86**, 223–235.
12. Patterson S.E. 2001. Cutting loose. Abscission and dehiscence in *Arabidopsis*. *Plant Physiol.* **126**, 494–500.
13. Flors V., de la O. Leyva M., Vicedo B., Finiti I., Real M.D., Garcia-Agustin P., Bennett A.B., Gonzalez-Bosch Carmen. 2007. Absence of the endo-β-1,4-D-glucanases Cel1 and Cel2 reduce susceptibility to *Botrytis cinerea* in tomato. *Plant J.* **52**, 1027–1040.
14. Libertini E., Li Y., McQueen-Mason S.J. 2004. Phylogenetic analysis of the plant endo-β-1,4-glucanase gene family. *J. Mol. Evol.* **58**, 506–515.
15. Urbanowicz B.R., Catala C., Irwin D., Wilson D.B., Ripoll D.R., Rose J.K.C. 2007. A tomato endo-β-1,4-glucanase, SlCel9C1, represents a distinct subclass with a new family of carbohydrate binding modules [CBM49]. *J. Biol. Chem* . **282**, 12066–12074.
16. Peng L.C., Kawagoe Y., Hogan P., Delmer D. 2002. Sitosterol-b-glucoside as primer for cellulose synthesis in plants. *Science.* **295**, 147–150.
17. Mølhøj M., Johansen B., Ulvskov P., Borkhardt B. 2001. Two *Arabidopsis thaliana* genes, *KOR2* and *KOR3*, which encode membrane-anchored endo-1,4-β-D-glucanases, are differentially expressed in developing leaf trichomes and their support cells. *Plant Mol. Biol.* **46**, 263–275.
18. Shani Z., Dekel M., Tsabary G., Shoseyov O. 1997. Cloning and characterization of elongation specific endo-beta-1,4-glucanase (Cel1) from *Arabidopsis thaliana*. *Plant Mol. Biol.* **34**, 837–842.
19. Shani Z., Dekel M., Tsabary G., Goren R., Shoseyov O. 2004. Growth enhancement of transgenic plants by overexpression of *Arabidopsis thaliana* endo1,4-β-glucanase (Cel1). *Plant Mol. Biol.* **14**, 321–330.
20. Shani Z., Dekel M., Roiz L., Horowitz M., Kolosovski N., Lapidot S., Alkan S., Koltai H., Tsabary G., Goren R., Shoseyov Oded. 2006. Expression of endo-1,4-endoglucanase (Cel1) in *Arabidopsis thaliana* is associated with plant growth, xylem development and cell wall thickening. *Plant Cell Rep.* **25**, 1067–1074.
21. Tsabary G., Shani Z., Roiz L., Levy I., Riov J., Shoseyov O. 2003. Abnormal 'wrinkled' cell walls and retarded development of transgenic *Arabidopsis thaliana* plants expressing endo-1,4-β-glucanase (Cel1) antisense. *Plant Mol. Biol.* **51**, 213–224.
22. del Campillo1 E., Abdel-Aziz A., Crawford D., Patterson S.E. 2004. Root cap specific expression of an endo-β-1,4-D-glucanase cellulase, a new marker to study root development in *Arabidopsis*. *Plant Mol. Biol.* **56**, 309–323.
23. Murashige T., Skoog F. 1962. A revised medium for rapid growth and bioassays with tobacco tissue culture. *Physiol. Plant.* **15**, 473–497.
24. Jefferson R.A., Kavanagh T.A., Bevan M.W. 1987. GUS fusions, beta-glucuronidase as a sensitive and versatile gene fusion marker in higher plants. *EMBO J.* **6**, 3901–3907.
25. Clough S.J., Bent A.F. 1998. Floral dip, a simplified method for *Agrobacterium*-mediated transformation of *Arabidopsis thaliana*. *Plant J.* **16**, 735–743.
26. Li H., Lin Y., Heath R.M., Zhu M.X., Yang Z. 1999. Control of pollen tube tip growth by a Rop GTPase-dependent pathway that leads to tip-localized calcium influx. *Plant Cell.* **11**, 1731–1742.
27. Palanivelu R., Brass L., Edlund A.F., Pruess D. 2003. Pollen tube growth and guidance is regulated by *POP2*, an *Arabidopsis* gene that controls GABA levels. *Cell.* **114**, 47–59.
28. Smyth D.R., Bowman J.L., Meyerowitz E.M. 1990. Early flower development in *Arabidopsis*. *Plant Cell.* **2**, 755–767.
29. Schneitz K., Hülskamp M., Pruitt R.E. 1995. Wild-type ovule development in *Arabidopsis thaliana*. A light microscope study of cleared whole-mount tissue. *Plant J.* **7**, 731–749.
30. Winter D., Vinegar B., Nahal H., Ammar R., Wilson G.V., Provart N.J. 2007. An 'electronic fluorescent pictograph' browser for exploring and analyzing large-scale biological data sets. *PloS ONE.* **2**, e718..
31. Yu H.J., Hogan P., Sundaresan V. 2005. Analysis of the female gametophyte transcriptome of *Arabidopsis* by comparative expression profiling. *Plant Physiol.* **139**, 1853–1869.
32. Tung C.W., Dwyer K.G., Nasrallah M.E., Nasrallah J.B. 2005. Genome-wide identification of genes expressed in *Arabidopsis* pistils specifically along the path of pollen tube growth. *Plant Physiol.* **138**, 977–989.
33. Jiang L., Yang S.L., Xie L.F., Puah C.S., Zhang X.Q., Yang W.C., Sundaresan V., Ye D. 2005. *VANGUARD1* encodes a pectin methylesterase that enhances pollen tube growth in the *Arabidopsis* style and transmitting tract. *Plant Cell.* **17**, 584–596.
34. Takahashi J., Rudsander U.J., Hedenstrom M. 2009. KORRIGAN1 and its aspen homolog PttCel9A1 decrease cellulose crystallinity in *Arabidopsis* stems. *Plant Cell Physiol.* **50**, 1099–1115.
35. Skinner D.J., Hill T.A., Gasser C.S. 2004. Regulation of ovule development. *Plant Cell.* **16**, S32–S45.
36. Pagnussat G.C., Alandete-Saez M., Bowman J.L., Sundaresan V. 2009. Auxin-dependent patterning and gamete specification in the *Arabidopsis* female gametophyte. *Science.* **324**, 1684–1689.
37. Yang W.C., Shi D.Q., Chen Y.H. 2010. Female gametophyte development in flowering plants. *Annu. Rev. Plant Biol.* **61**, 27.1–27.20.
38. Coimbra S., Almeida J., Junqueira V., Costa M., Pereira L.G. 2007. Arabinogalactan proteins as molecular markers in *Arabidopsis thaliana* sexual reproduction. *J. Exp. Bot.* **58**, 4027–4035.